Interactions between Poly(acrylic acid) and Sodium Dodecyl Sulfate: Isothermal Titration Calorimetric and Surfactant Ion-Selective Electrode Studies

C. Wang and K. C. Tam*

School of Mechanical and Production Engineering, Division of Chemical & Biomolecular Engineering, College of Engineering, Nanyang Technological University, 50 Nanyang Avenue, Singapore 639798

Received: October 5, 2004; In Final Form: January 5, 2005

Interaction between a monodispersed poly(acrylic acid) (PAA) (M_W = 5670 g/mol, M_w/M_n = 1.02) with sodium dodecyl sulfate (SDS) was investigated using isothermal titration calorimetry (ITC), ion-selective electrode (ISE), and dynamic light scattering measurements. Contrary to previous studies, we report for the first time evidence of interaction between SDS and PAA when the degree of neutralization (α) of PAA is lower than 0.2. Hydrocarbon chains of SDS cooperatively bind to apolar segments of PAA driven by hydrophobic interaction. The interaction is both enthalpy and entropy favored (ΔH is negative but ΔS is positive). In 0.05 wt % PAA solution, the SDS concentration corresponding to the onset of binding (i.e., CAC) is ~2.4 mM and the saturation concentration (i.e., C_S) is ~13.3 mM when $\alpha = 0$. When PAA was neutralized and ionized, the binding was hindered by the enhanced electrostatic repulsion between negatively charged SDS and PAA chains and improved solubility of the polymer. With increasing α to 0.2, CAC increases to ~6.2 mM, C_S drops to 8.6 mM, and the interaction is significantly weakened where the amount of bound SDS on PAA is reduced considerably. The values of CAC and C_S derived from different techniques are in good agreement. The binding results in the formation of mixed micelles on apolar PAA coils, which then expands and dissociates into single PAA chains. The majority of unneutralized PAA molecules exist as single polymer chains stabilized by bound SDS micelles in solution after the saturation concentration.

Introduction

Interactions between polyelectrolytes and ionic surfactants in aqueous solutions have attracted increasing attention because of their complex behaviors and potential applications in rheological control, detergency, and pharmaceutical formulations. A number of research groups have devoted significant attention in advancing the understanding on the mechanisms, thermodynamics, phase behavior, and structure of the polymer/surfactant complex.[1−14]

Most of the studies focused on the interactions between oppositely charged polyelectrolytes and surfactants, where the strong electrostatic interaction is clearly observable and occurs at concentration several orders of magnitude below the critical micelle concentration (cmc).[1−5,8,11−13] The interactions between cationic surfactants (e.g., alkyltrimethylammonium) and anionic polyacids have been extensively studied. It was found that surfactant molecule binds to carboxylate sites on polymer chains in stoichiometric proportions and the polymer/surfactant complex precipitates when the amounts of positive and negative charges are equivalent.[1,3,13−18] On the other hand, interactions between an anionic surfactant such as sodium dodecyl sulfate (SDS) and cationic polymers such as proteins and cationic cellulose were also examined.[3,15,19] These interactions are electrostatic driven and they alter the conformation of the protein molecules from a random structure to a folded-helix.[3,19] Such interaction is believed to be an ion-exchange process induced by strong electrostatic forces, reinforced by the aggregation of hydrophobic alkyl chains of bound surfactant molecules. Generally, it is accepted that the electrostatic attraction is the primary driving force in the binding between oppositely charged polymer and surfactant, which is reinforced by a cooperative aggregation of bound surfactant molecules.[1,3,9,11−13,16,17]

The interactions between weak polyelectrolytes with oppositely charged surfactants were also studied. It was found that the interactions are governed by several factors such as polymer charge density, chain flexibility, ionic strength, and chemical nature of charged sites.[1,2,18,20−28] It was also reported that forces other than the electrostatic attraction, such as hydrogen bonding[25−27] and hydrophobic interaction[21−23,28] are responsible for the binding of these surfactants to weakly charged polyelectrolytes.

However, interactions between polyelectrolytes and surfactants of the same charge are less extensively studied because the interaction is believed to be weak or nonexistence.[29−31] Zana and co-workers proposed the complexation mechanism between SDS and pluronic-PAA at low pH.[29] Bromberg et al. studied the interactions between hydrophobically modified PAA (pluronic-PAA) and SDS using surface tension and rheology measurements and they found that SDS binds to the propylene oxide (PPO) segment of the polymer and hinders the formation of inter-polymerchain association (gelation).[31] Eisenberg and co-workers studied the interaction between SDS and polystyrene-*b*-poly(acrylic acid) block copolymer (PS-*b*-PAA) in a dioxane−water mixture.[32] They observed that the ionic headgroups of SDS repel the charged PAA chains and the hydrocarbon chains of SDS partition into the PS core of the polymer aggregates, and this induces morphological transformation.[32] The interactions between SDS and pyrene (Py) labeled poly(carboxylic acid)s have also been investigated by fluorescence in recent years.[33,34] The interaction between SDS and PAA was studied using the fluorescence probe (Py) and label (PAA-BuPy)

* To whom correspondence should be addressed. Fax: 65-6791-1859. E-mail: mkctam@ntu.edu.sg.

10.1021/jp045468t CCC: $30.25
Published on Web 02/26/2005

techniques.[33] The authors revealed that PAA/SDS complex is formed at low pH condition (<2.4); the complexation is disrupted with increasing pH and ceased completely when PAA is fully neutralized.[33] Anghel el al. investigated the interaction between SDS and Py labeled PAA using steady-state fluorescence spectroscopy.[34] SDS was found to cooperatively bind to labeled PAA driven by hydrophobic interaction at pH = 3, which consequently uncoils the PAA aggregates. Moreover, the value of critical aggregation concentration (CAC) decreases with increase of salt concentration, however, it is independent of the molar mass of PAA.[34]

It is noted that both hydrophobic modification and Py-labeling of PAA significantly enhances the overall hydrophobicity of the polymer, which promotes its interaction with SDS. Whether SDS binds to unmodified PAA is still a scientific issue that remains to be resolved, and which this paper seeks to address. We present in this paper a quantitative study on the interaction between SDS and unmodified PAA at different degrees of neutralization (α), using isothermal titration calorimetry (ITC), surfactant ion selective electrode (ISE) and dynamic light scattering (DLS) techniques. ITC is one of the most sensitive techniques that permit the direct measurement of thermodynamic changes in the course of binding and micellization.[6,7,16,17,27,28] Thermodynamic parameters such as enthalpy (ΔH), entropy (ΔS) and Gibbs energy (ΔG) can be extracted from ITC measurements and they are critical to the understanding of polymer/surfactant interactions.[16,17,27,28] The equilibrium properties of polymer/surfactant binding was quantified by electromotive force measurements (EMF) using SDS selective electrode. EMF provides the most direct and convenient way to determine the binding isotherms by measuring the concentration of free surfactant molecules in polymer solutions.[6,7,10,23,35−39] EMF measurements on varieties of polymer/surfactant systems, including nonionic polymer/anionic surfactant, nonionic polymer/cationic surfactant and oppositely charged polymer/surfactant have been extensively studied by Wyn-Jones and co-workers.[6,7,10,35−39] Moreover, the combination of ITC and EMF allows accurate identification of the critical concentrations, such as CAC, saturation concentration (C_S), and critical micellization concentration of surfactant in the polymer solution. It is hoped that this study can provide a better understanding on the complexation mechanism between SDS and PAA at different α.

Experimental Details

Materials. The PAA with M_W = 5,670 g/mol and polydispersity index (PDI) of 1.02 was obtained from Polymer Source Co. (Montreal, CA) A standard 1 M NaOH solution from Merck was used to adjust the degree of neutralization of PAA. The anionic surfactant, sodium dodecyl sulfate was obtained from BDH Lab Supplies (SDS, >99%) and used as received without further purification. Water was obtained from the Millipore Alpha-Q water purification system, which has a resistivity of 18.2 $\mu\Omega$ cm.

Isothermal Titration Calorimetry. The microcalorimetric study was carried out using a Microcal isothermal titration calorimeter (ITC). This power compensation, differential instrument was previously described in detail by Wiseman et al.[40,41] It has a reference and a sample cell of approximately 1.35 mL each, and the cells are both insulated by an adiabatic shield. The titration was carried out at 25.0 ± 0.02 °C, by injecting 200 mM SDS solution from a 250 μL injection syringe into the sample cell filled with 0.05 wt % polymer solution. The syringe is tailored-made such that the tip acts as a blade-type stirrer to ensure an optimum mixing efficiency at 400 rpm. The heat evolved or absorbed by each injection in the course of titration is directly measured by the ITC unit, producing the raw heat signal, also known as cell feedback (CFB). Integration of the each CFB gives the differential enthalpy curve for the titration.

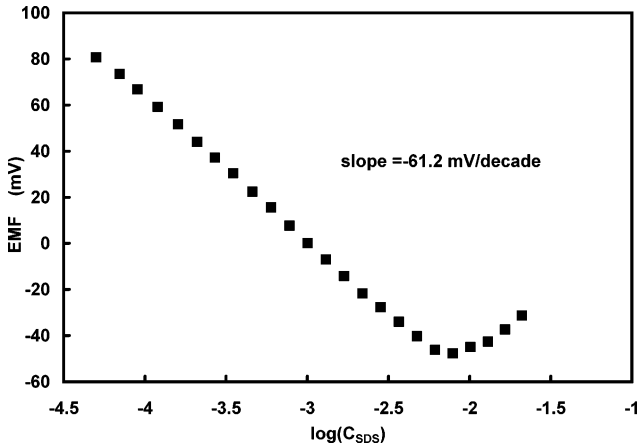

Figure 1. Calibration curve for SDS selective electrode in 10^{-4} M NaBr at 298 K.

Surfactant Ion Selective Electrode. A surfactant membrane electrode selective to SDS constructed in the laboratory at Salford University was used to determine the surfactant monomer concentrations by measuring their EMF relative to a commercial bromide electrode. The construction of the electrode has been described previously.[42,43] The EMF was measured and recorded by the Radiometer ABU93 triburet titration system with a built-in microvoltmeter. The EMF measurements were performed at 25 °C. A 200 mM SDS solution was added dropwise to a rapidly stirred 25 mL 0.05 wt % polymer solution in 10^{-4} M NaBr every 5 min, followed by the determination of EMF when the equilibrium was reached. The calibration curves (dependence of EMF on log(C_{SDS})) obtained from titrating 0.1 M SDS solution into 10^{-4} M NaBr solution at 298 K is shown in Figure 1. The calibration curve exhibits an inflection point at $C_{SDS} \sim 7.9$ mM, signifying the cmc of SDS. Below the cmc, the plot is linear with a slope of −61.22 mV/decade that indicates Nernstian behavior.

Dynamic Laser Light Scattering. The dynamic laser light scattering experiments were conducted using the Brookhaven MAS (multiangle sizing option) dynamic light scattering system. A 5−15 mW solid-state laser of wavelength λ_0 = 671 nm was used as the light source. The time correlation function of the scattered intensity $G_2(t)$, which is defined as $G_2(t) = I(t)I(t + \Delta t)$ where $I(t)$ is the intensity at time t and Δt is the lag time, is analyzed using the inverse Laplace transformation technique (REPES for our case) to produce the distribution function of decay times. Thus, the apparent hydrodynamic radius can be determined from the decay rate via the Stokes−Einstein equation:

$$R_h = \frac{kTq^2}{6\pi\eta\Gamma} \quad (1)$$

where k is the Boltzmann constant, q is the scattering vector ($q = (4\pi n \sin(\theta/2))/\lambda$, where n is the refractive index of solvent, θ is the scattering angle and λ is the wavelength of the incident laser light in a vacuum), η is the solvent viscosity, and Γ is the decay rate. Several measurements were performed at 90° for a sample to obtain an average hydrodynamic radius and the variation in the R_h values was found to be small.

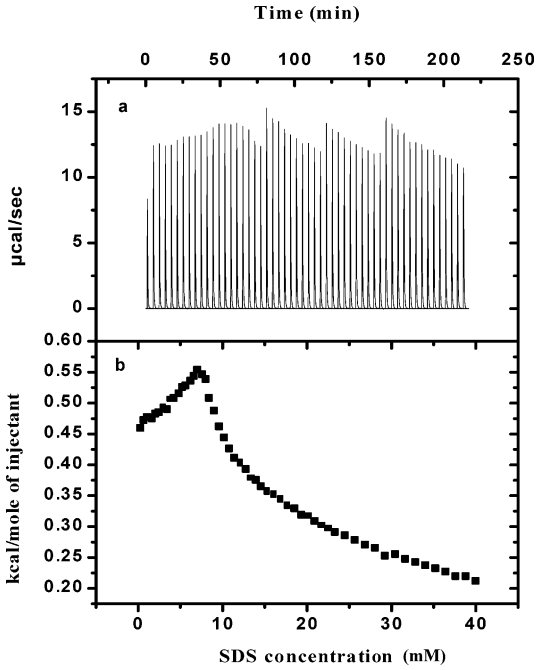

Figure 2. Calorimetric titration of 200 mM SDS into 0.05 wt % solution of PAA at $\alpha = 0.8$: (a) thermogram showing cell feedback (CFB) vs time; (b) differential enthalpic curves vs the SDS concentration.

Results and Discussion

Isothermal Titration Calorimetric Study. Isothermal calorimetric titrations were conducted by stepwise injections of 200 mM SDS solution into the sample cell filled with 0.05 wt % (monomer concentration is 6.94 mM) PAA at different degrees of neutralization (α) ranging from 0 to 1.0. The α values were determined using potentiometric titration of the PAA. The definition of α is given by the following equation:

$$\alpha = \frac{[\mathrm{NaOH}] + [\mathrm{H^+}] - [\mathrm{OH^-}]}{C_{\mathrm{COOH}}} \qquad (2)$$

where [NaOH], [H^+], and [OH^-] are the molarities of NaOH, free hydrogen ion, and hydroxide ion respectively in the course of potentiometric titration, and C_{COOH} is the total concentration of carboxylic groups expressed in moles per liter. With this definition, "$\alpha = 0$" represents the state of unneutralized PAA where all the carboxylic groups remain uncharged; and "$\alpha = 1$" corresponds to the state of fully neutralized (ionized) PAA.

The thermogram demonstrating the cell feedback (CFB) of the titrations in the PAA solutions at $\alpha = 0.8$ is shown in Figure 2a, where the sudden changes on heat signal at injection nos. 2, 20, 30, and 40 are caused by the increase in the injection volume. Integration of the area of CFB gives the differential enthalpy curve as shown in Figure 2b. The differential enthalpy curves of titrations at $\alpha = 0$, 0.1, 0.15, 0.2, 0.25, 0.4, and 0.8 were plotted together with the dilution curve (titration of SDS into water) in Figure 3. The inflection point on the enthalpic dilution curve represents the cmc of SDS, which is 8.6 mM and is close to the value reported in the literature.

At $\alpha \leq 0.2$, the enthalpy profiles corresponding to the titration of SDS to PAA exhibit an exothermic peak over a predefined range of SDS concentrations. The exothermic peak diminishes with increase of α and it completely disappears when α exceeds 0.2. When $\alpha > 0.2$, the titration curves of SDS into PAA are identical with the dilution curve, indicating that there is no interaction between SDS and PAA at higher α. It is expected

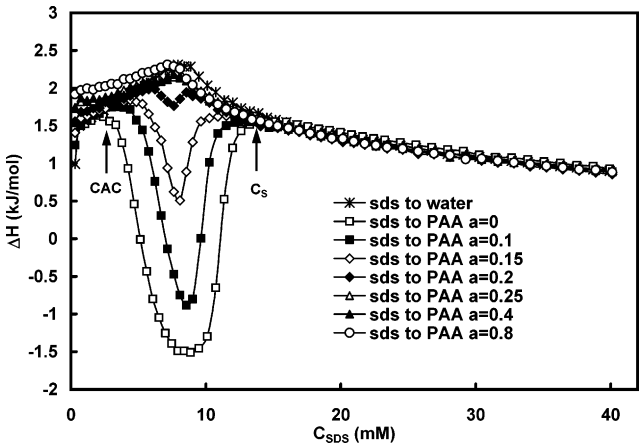

Figure 3. Differential enthalpy curves for titrating 200 mM SDS into 0.05 wt % solutions of PAA at different α: (□) $\alpha = 0$; (■) $\alpha = 0.1$; (◇) $\alpha = 0.15$; (◆) $\alpha = 0.2$; (△) $\alpha = 0.25$; (▲) $\alpha = 0.4$; (○) $\alpha = 0.8$; (∗) dilution curve.

TABLE 1: CAC, C_S, and Thermodynamic Parameters Obtained from Calorimetric Titration of SDS into 0.05 wt % PAA at $\alpha = 0$, 0.1, 0.15, and 0.2

α	CAC (mM)	C_S (mM)	ΔH (kJ/mol)	ΔG (kJ/mol)	ΔS (J/mol K)
0.00	2.4	13.3	−2.04	−27.65	85.9
0.10	3.9	12.1	−1.63	−25.42	79.8
0.15	4.8	10.3	−1.27	−24.47	77.9
0.20	6.2	8.60	−0.88	−23.30	75.2

that SDS cannot interact with neutralized or partially neutralized PAA because they both possess negative charges and the strong electrostatic repulsion prevents the surfactant from binding to the polymer.

The most interesting feature of the titration curves shown in Figure 3 is the exothermic peak observed at $\alpha \leq 0.2$, suggesting that SDS binds to PAA when α is sufficiently low. We believe this is the first reported evidence of binding of SDS to PAA at low degree of neutralization. The critical concentrations for the binding can be determined from the enthalpy profiles, which are indicated by the arrows in Figure 3. The enthalpic binding profile diverges from the dilution curve at a critical SDS concentration (termed critical aggregation concentration—CAC) to produce an exothermic peak. Thereafter it ceases and merges with the dilution curve at another critical SDS concentration, corresponding to the saturation of PAA with bound SDS, namely C_S. The values of CAC, C_S, and other thermodynamic parameters extracted from enthalpy curves are summarized in Table 1. The enthalpy change after subtracting the dilution heat obtained from the titration of SDS to PAA at $\alpha \leq 0.2$ is shown in Figure 4. With increasing α from 0 to 0.2, CAC increases from C_{SDS} of 2.4 to 6.2 mM, C_S decreases from C_{SDS} of 13.3 to 8.6 mM, and the amplitude of the exothermic peak decreases from −3.79 to −0.45 kJ/mol. These indicate that the binding is weakened and the amount of bound SDS on PAA decreases with increasing α. This is reasonable because the binding is opposed by the electrostatic repulsion between SDS and PAA, which becomes stronger at high α. When α exceeds 0.2, the electrostatic repulsion completely overwhelms the interaction force between SDS and MAA and the binding ceases.

The hydrophobic interaction is considered to be the primary driving force for the observed binding interaction. At $\alpha \leq 0.2$, the majority of the carboxylic groups on PAA remain uncharged and the polymer backbones are fairly hydrophobic.[13,21,27,44] Several polymer chains may aggregate with each other to form a compact random coil, and the interaction between the

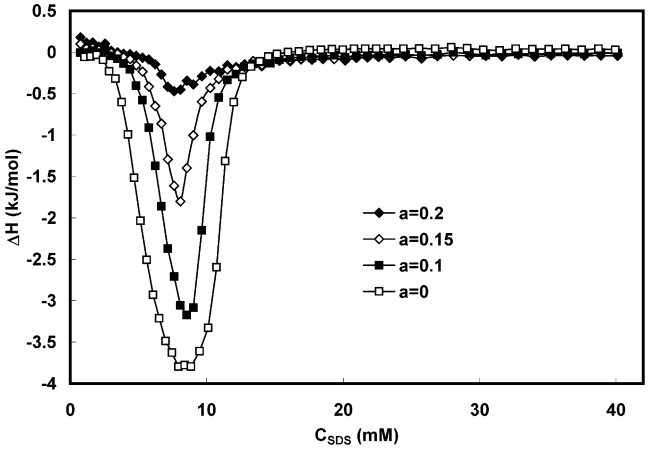

Figure 4. Differential enthalpies by subtracting the dilution heat obtained from titrating 200 mM SDS into 0.05 wt % solutions of PAA at different α: (□) α = 0, (■) α = 0.1, (◇) α = 0.15, (◆) α = 0.2.

hydrophobic domains within these aggregates and hydrocarbon chains of SDS is responsible for the binding.[13,21,27,44] The Gibbs energy of the binding was determined by applying the semi-quantitative approach based on the pseudo-phase separation model. The model assumes that the micelles exist as a separate microphase, in equilibrium with the solution containing the solvent and free surfactant, and the composition of the phases are independent of the phase volume.[3,16,17,45,46] The Gibbs energy is expressed as

$$\Delta G = (1 + K)RT \ln[\mathrm{CAC}] \tag{3}$$

where K is the effective micellar charge fraction with a value of 0.85 for SDS,[45,46] and CAC is the critical aggregation concentration obtained from the enthalpic binding profile. The apparent enthalpy of binding was derived from the integration of the exothermic peak normalized by the SDS concentration. Once the values of ΔH and ΔG have been obtained, the entropy ΔS can be determined from eq 4:

$$\Delta S = \frac{\Delta H - \Delta G}{T} \tag{4}$$

The values of enthalpy ΔH, entropy ΔS, and Gibbs energy ΔG are summarized in Table 1. The thermodynamic parameters suggest that both enthalpy and entropy are favorable for the binding. The binding is exothermic and the negative ΔH is attributed to the energy evolved due to the binding of SDS onto PAA. The entropy change ΔS is positive and this is attributed to the expelled water molecules from disrupted solvent cages due to hydrophobic binding, and the values of ΔS are essentially independent of α. It is noted that the absolute value of Gibbs energy decreases from −27.65 to −23.30 kJ/mol when α increases from 0 to 0.2, indicating that binding is unfavorable with the ionization of PAA due to weakened hydrophobic attraction and strengthened electrostatic repulsion between PAA and SDS.

Electromotive Force (EMF) Study. To verify the binding mechanism elucidated from ITC studies and to obtain the binding isotherms for SDS to PAA at different α, EMF measurements were conducted. Free monomeric SDS concentration was determined potentiometrically using a surfactant membrane electrode selective to SDS against a commercial Br^- electrode as a reference. The plots of EMF against logarithmic of SDS concentration in solutions of 0.05 wt % PAA at α = 0, 0.1, and 0.4 together with the calibration curve are shown in Figure 5.

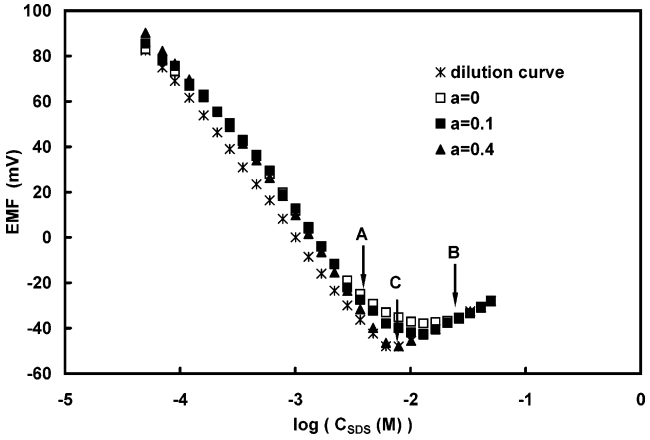

Figure 5. EMF determined using SDS selective electrode for the titration of SDS to 0.05 wt % solutions of PAA at different α in 10^{-4} M NaBr: (□) α = 0; (■) α = 0.1; (▲) α = 0.4; (∗) dilution curve.

The EMF curves obtained in the presence of PAA at α = 0 diverges from the Nernstian behavior at a critical SDS concentration ∼2.4 mM (marked by arrow "A" in Figure 5), indicating the CAC, namely the onset of cooperative binding of SDS to unneutralized or partially neutralized PAA. With further addition of SDS to ∼13.3 mM, the binding curves merge with the calibration curve (marked by arrow "B" in Figure 5), corresponding to C_S, namely the saturation concentration when the binding ceases. The inflection point at C_{SDS} ∼10 mM (marked by arrow "C" in Figure 5) indicating the micellization of SDS occurs prior to the merging of the binding and calibration curves, suggesting that free SDS micelles are formed before the saturation of PAA. This concentration is also known as the second critical micelle concentration in the presence of polymer, namely C_m. When α was increased to 0.1, the binding curve resembles that at α = 0. However, the CAC increases to ∼4.0 mM, C_S decreases to 12.0 mM, and the EMF values within the binding region becomes lower (i.e., SDS monomer concentration is higher) compared to that at α = 0. This suggests that the binding is opposed by the ionization of PAA that reduces the hydrophobicity of the polymer and strengthens the electrostatic repulsion between PAA chains and SDS. When α was increased to 0.4, the EMF curve exhibits identical trend with the calibration curve, and the CAC was not observed, suggesting that SDS has negligible interaction with PAA at α ≥ 0.4. Moreover, the critical concentrations (CAC and C_S) determined from ITC and EMF measurements are fairly similar, confirming that there is significant interaction between SDS and PAA at low α and the binding profiles obtained from different techniques are in good agreement.

Ideally, the EMF curves obtained in the presence of polymer should merge with the calibration curve before CAC. However, they diverge from the calibration curve as shown in Figure 5. The difference between the binding and calibration curves before CAC does not correspond to binding because it persists even when α is higher than 0.4, where the polymer are sufficiently ionized and the hydrophobic binding ceases. Thus, it is believed the difference is caused by the absorbance of polymer on the membrane of the electrode which affects the relative magnitude of the millivolts.

The binding fractions determined from the absorption curves at α = 0, 0.1, and 0.4 were plotted against the total SDS concentration in Figure 6. The binding fraction β is defined as

$$\beta = \frac{C_b}{C_t} \tag{5}$$

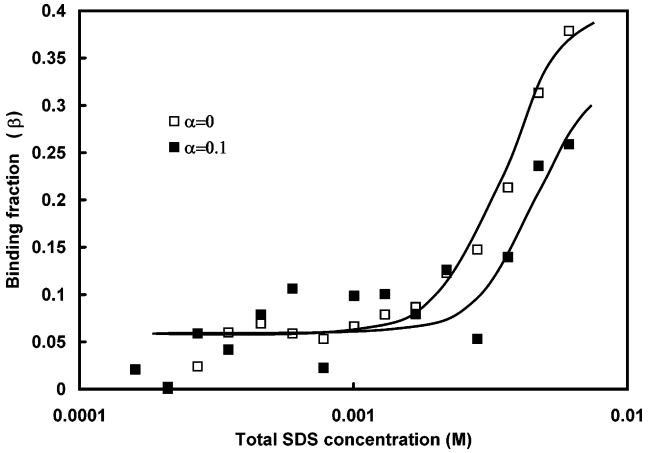

Figure 6. Binding fraction (C_b/C_t) as a function of SDS concentration in 0.05 wt % solution of PAA at $\alpha = 0$ (□) and 0.1 (■).

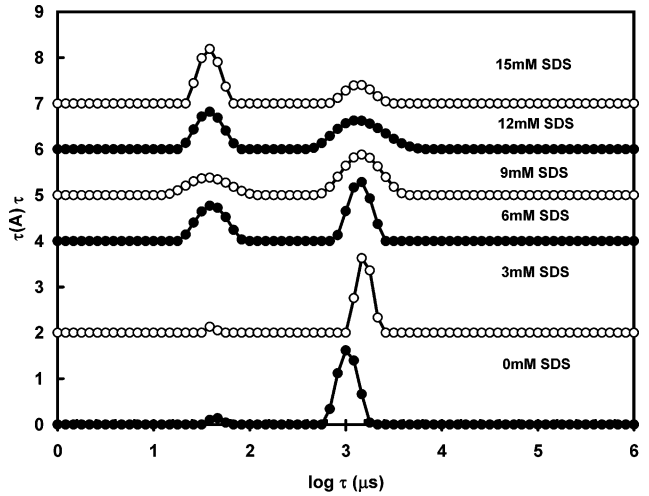

Figure 7. Relaxation time distribution functions of 0.05 wt % PAA at $\alpha = 0$ with presence of different amount of SDS (varies from 0 to 15 mM) measured at 298 K and 90°.

where C_b is the concentration of polymer bound surfactant and C_t is the total surfactant concentration. It is noted that the binding fraction is only valid when the total SDS concentration is lower than C_m. Initially the binding fraction is less than 5%, suggesting that most of the SDS molecules exist as free monomers. With continuous addition of surfactant and when its concentration reaches a critical value (i.e., CAC), the binding fraction soars to >40%, signaling the onset of the binding. The CAC at $\alpha = 0$ is apparently lower than that at $\alpha = 0.1$ due to a stronger hydrophobic interaction when the polymer charge density is smaller. At $C_{SDS} \sim$6mM, the binding fractions are 37.8% and 25.8% for $\alpha = 0$ and $\alpha = 0.1$, respectively; thus we determined that each PAA chain (M_w = 5670 g/mol, PDI = 1.02) binds approximately 26 and 18 SDS molecules at $\alpha = 0$ and 0.1, respectively.

Dynamic Light Scattering Study. To verify the binding mechanism of SDS to unneutralized PAA derived from ITC and EMF studies, dynamic light scattering was performed for SDS/PAA mixture at $\alpha = 0$. The concentration of unneutralized PAA was kept at 0.05 wt %, where the SDS concentration was varied from 0 to 15 mM covering the entire binding regime, and all the measurements were conducted in 0.1 M NaCl solutions. The relaxation time distribution functions of 0.05 wt % unneutralized PAA with added SDS (from 0 to 15 mM) measured at 90° are shown in Figure 7. The relaxation time distribution functions for the PAA/SDS mixture were also measured at different scattering angles (from 50 to 90° at 10° interval) in order to determine the dependence of decay rate Γ on q^2. It is found that Γ exhibits good linear relationship with q^2, confirming that the distribution functions are caused by the translational diffusion of polymer or polymer/surfactant complex.

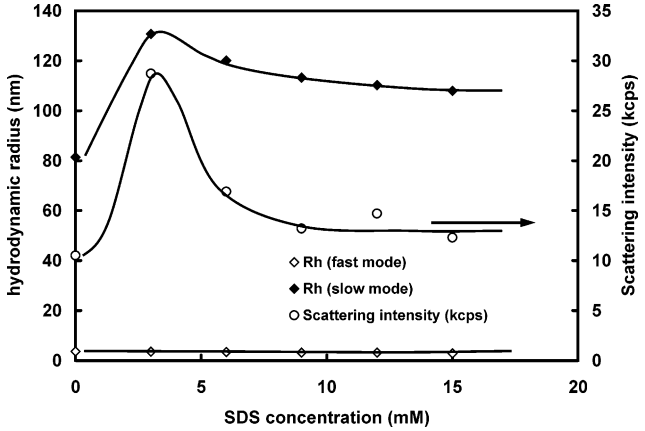

Figure 8. Dependence of R_h^{app} and scattering intensity on SDS concentration in 0.05 wt % PAA at $\alpha = 0$: (◇) R_h of single PAA chain; (◆) R_h of coiled PAA; (○) overall scattering intensity.

The unneutralized PAA is fairly hydrophobic and several polymer chains may aggregate with each other to form randomly coiled aggregates. The distribution function of PAA at $\alpha = 0$ in the absence of SDS is bimodal, the fast mode may represent the single polymer chains and the slow mode characterizes the aggregates. With an increase in the SDS concentration to 3 mM, the scattering intensity increases from 10.5 to 28.7 kcps, where the distribution function of the fast mode remains essentially unchanged and the distribution function of the slow mode shifts to a higher relaxation time. This corresponds to the formation of SDS micelles on apolar segments of PAA that swells the aggregates. With further increase of SDS concentration from 3 to 15 mM, the fast mode becomes more significant, and the slow mode shifts slightly to lower relaxation time and the scattering intensity decreases from 28.7 to 12.3 kcps. This is attributed to the dissociation of PAA aggregates bound with SDS micelles, which greatly increases the amount of single polymer chains in solution and in turn decreases the size of aggregates.

The hydrodynamic radius (R_h^{app}) calculated from the relaxation times and scattering intensity were plotted against SDS concentration in Figure 8. The hydrodynamic radius of single PAA chains (fast mode) in the absence of surfactant is approximately 3 nm, and it is essentially independent of SDS concentration during the entire course of binding. The hydrodynamic radius of the aggregates (slow mode) without addition of SDS is approximately 81 nm, and it increases to 131 nm when SDS concentration increases to 3 mM, corresponding to the expansion of PAA aggregates caused by the electrostatic repulsion introduced by bound SDS micelles. With an increase in the SDS concentration to 6 mM, the hydrodynamic radius of the aggregates with bound surfactant decreases to 121 nm and the scattering intensity also drops. This suggests that some PAA chains bound with SDS micelles are expelled from the aggregates and are stabilized in solution, which dissociates the aggregates, thereby reduces the size of aggregates and significantly increases the amount of single PAA chains (as shown in Figure 7). With further increase of the SDS concentration to 15 mM, the hydrodynamic radius of the aggregates with bound surfactant slightly decreases to 108 nm, and more PAA chains

are disassociated from the aggregates and stabilized in solution by bound SDS micelles.

Conclusions

We observed binding of SDS to PAA chains at degree of neutralization less than 0.2. An exothermic peak was observed in the enthalpy curve, where it becomes less significant with increasing α and completely disappears when α exceeds 0.2. The peak characterizes the binding of SDS to apolar segment of unneutralized PAA coils driven by hydrophobic interaction. The interaction is both ΔH and ΔS favorable, where the negative ΔH indicates the hydrophobic interaction and the entropy gain is attributed to the disruption of water structure upon the formation of SDS micelles on PAA.

In 0.05 wt % PAA solution, the SDS concentration corresponding to the onset of binding (CAC) is ~2.4 mM and the saturation concentration (C_S) is ~13.3 mM when $\alpha = 0$. With increasing α to 0.2, CAC increases to ~6.2 mM, C_S decreases to 8.6 mM, the interaction is significantly weakened and the amount of bound SDS on PAA is considerably reduced.

Dynamic light scattering study demonstrates that the size of PAA coil increases initially and then decreases upon addition of SDS, suggesting the structural transformation of PAA coils induced by the binding (complexation). The structural transformation is related to the expansion caused by electrostatic repulsion between bound charged SDS micelles, which is followed by the dissociation of PAA coils. When the polymer is saturated with bound SDS, the majority of PAA uncoils to form single polymer chains stabilized by several bound SDS micelles.

Acknowledgment. We would like to express our gratitude to Professor E. Wyn-Jones from the University of Salford for providing us with the surfactant ion-selective electrodes and for his helpful advice on the experimental setup and data analysis of the EMF measurements.

References and Notes

(1) Hayakawa, K.; Kwak, J. C. T. *J. Phys. Chem.* **1982**, *86*, 3866.
(2) Hayakawa, K.; Santerre, J. P.; Kwak, J. C. T. *Macromolecules* **1983**, *16* (10), 1642.
(3) Goddard, E. D. In *Interactions of Surfactants with Polymers and Proteins*; Goddard, E. D., Ananthapadmanabhan, K. P., Eds.; CRC Press: Boca Raton, FL; 1993; p 171.
(4) Anthony, O.; Zana, R. *Langmuir* **1996**, *12*, 1967.
(5) Khokhlov, A. R.; Dormidontova, E. E. *Phys.-Usp.* **1997**, *40* (2), 109.
(6) Ghoreishi, S. M.; Fox, G. A.; Bloor, D. M.; Holzwarth, J. F.; Wyn-Jones, E. *Langmuir* **1999**, *15*, 5474.
(7) Li, Y.; Ghoreishi, S. M.; Warr, J.; Bloor, D. M.; Holzwarth, J. F.; Wyn-Jones, E. *Langmuir* **1999**, *15*, 6326.
(8) Merta, J.; Stenius, P. *Colloids Surf. A* **1999**, *149*, 367.
(9) Konop, A. J.; Colly, R. H. *Langmuir* **1999**, *15*, 58.
(10) Ghoreishi, S. M.; Li, Y.; Holzwarth, J. F.; Khoshdel, E.; Warr, J.; Bloor, D. M.; Wyn-Jones, E. *Langmuir* **1999**, *15*, 1938.
(11) Ehtezazi, T.; Govender, T.; Stolink, S. *Pharm. Res.* **2000**, *17*, 871.
(12) Matulis, D.; Rouzina, L.; Bloomfield, V. A. *J. Mol. Biol.* **2000**, *296*, 1053.
(13) Fundin, J.; Hansson, P.; Brown, W.; Lidegran, I. *Macromolecules* **1997**, *30*, 1118.
(14) Hansson, P. *Langmuir* **2001**, *17*, 4167.
(15) Rodenhiser, A. P.; Kwak, J. C. T. Polymer-Surfactant System: Introduction and Overview. In *Polymer-Surfactant System.* New York: Marcel Dekker: 1998.
(16) Wang, C.; Tam, K. C. *Langmuir* **2002**, *18*, 6484−6490.
(17) Wang, C.; Tam, K. C.; Jenkins, R. D.; Tan, C. B. *J. Phys. Chem. B* **2003**, *107*, 4667.
(18) Chandar, P.; Somasundaran, P.; Turro, N. J. *Macromolecules* **1988**, *21*, 950.
(19) Shirahama, K. In *Polymer-Surfactant System*; Kwak, J. C. T., Ed.; Marcel Dekker: New York, 1998; p 143.
(20) Kosmella, S.; Kötz, J.; Shirahama, K.; Liu, J. J. *Phys. Chem. B* **1998**, *102*, 6459.
(21) Kiefer, J. J.; Somasundaran, P.; Ananthapadmanabhan, K. P. *Langmuir* **1993**, *9*, 1187.
(22) Kogej, K.; Theunissen, E.; Reynaers, H. *Langmuir* **2002**, *18*, 8799.
(23) Katsuura, H.; Kawamura, H.; Manabe, M.; Kawasaki, H.; Maeda, H. *Colloid Polym. Sci.* **2002**, *280*, 30.
(24) Shimizu, T. *Colloids Surf. A: Phys. Eng. Aspects* **1994**, *84*, 239.
(25) Yoshida, K.; Dubin, P. L. *Colloids Surf. A: Phys. Eng. Aspects* **1999**, *147*, 161.
(26) Anghel, D. F.; Saito, S.; Băran, A.; Iovescu, A. *Langmuir* **1998**, *14*, 5342.
(27) Wang, C.; Tam, K. C. *J. Phys. Chem. B* **2004**, *108*, 8976.
(28) Wang, C.; Tam, K. C.; Tan, C. B. *Langmuir* **2004**, *20*, 7933.
(29) Binana-Limbele, W.; Zana, R. *Colloids Surf.* **1986**, *21*, 483.
(30) Maltesh, C.; Somasundaran, P. *Colloids Surf.* **1992**, *69*, 167.
(31) Bromberg, L.; Temchenko, M.; Colby, R. H. *Langmuir* **2000**, *16*, 2609.
(32) Susan, E. B.; Eisenberg, A. *Langmuir* **2001**, *17*, 8341.
(33) Maltesh, C.; Somasundaran, P. *Langmuir* **1992**, *8*, 1992.
(34) Anghel, D. F.; Toca-Herrera, J. L.; Winnik, F. M.; Rettig, W.; Klitzing, R. V. *Langmuir* **2002**, *18*, 5600.
(35) Fox, G. J.; Bloor, D. M.; Holzwarth, J. F.; Wyn-Jones, E. *Langmuir* **1998**, *14*, 1026.
(36) Li, Y.; Bloor, D. M.; Wyn-Jones, E. *Langmuir* **1996**, *12*, 4476.
(37) Li, Y.; Xu, R.; Couderc, S.; Bloor, D. M.; Holzwarth, J. F.; Wyn-Jones, E. *Langmuir* **2001**, *17*, 5742.
(38) Xu, R.; Bloor, D. M. *Langmuir* **2000**, *16*, 9555.
(39) Thurn, T.; Couderc, S.; Sidhu, J.; Bloor, D. M.; Penfold, J.; Holzwarth, J. F.; Wyn-Jones, E. *Langmuir* **2002**, *18*, 9267.
(40) Wiseman, T.; Williston, S.; Brandts, J. F.; Lin, L. *Anal. Biochem.* **1989**, *179*, 131.
(41) Jelesarov, I.; Bosshard, H. R. *J. Mol. Recognit.* **1999**, *12*, 3.
(42) Wan-Badhi, W. A.; Wan-Yunus, W. M. Z.; Bloor, D. M.; Hall, D. G.; Wyn-Jones, E. *J. Chem. Soc., Faraday Trans.* **1993**, *89*, 2737.
(43) Xu, R. Ph.D. Dissertation, Salford University, Salford, U.K., 2002.
(44) Nagasawa, M.; Murase, T.; Kondo, K. *J. Phys. Chem.* **1965**, *69*, 4005.
(45) Wang, Y.; Han, B.; Yan, H.; Kwak, J. C. T. *Langmuir* **1997**, *13*, 3119.
(46) Linse, P.; Piculell, L.; Hansson, P. In *Polymer-Surfactant System*; Kwak, J. C. T., Ed.; Marcel Dekker: New York, 1998; p 193.